# Calibrating Evolution in the Tully-Fisher Relation

S. J. Kannappan, D. G. Fabricant

*Harvard-Smithsonian Center for Astrophysics, Cambridge, MA 02138*

and

M. Franx

*Leiden Observatory, Leiden, The Netherlands*

## ABSTRACT

We reevaluate evidence for luminosity evolution in the intermediate-redshift Tully-Fisher relation (TFR), focusing on the spatially resolved kinematic data sets of Vogt et al. (1997) and Simard & Pritchet (1998). We use low-$z$ data from the Nearby Field Galaxy Survey (NFGS) to match the intermediate-$z$ studies' sample selection criteria, analysis techniques, and data quality. The passively evolving disk galaxy sample of Vogt et al. shows no luminosity evolution within the errors, approximately confirming these authors' results. The [OII]-selected sample of Simard & Pritchet shows $\lesssim$0.5 mag of luminosity evolution, substantially less than the 1.5–2 mag originally reported; we trace about half of the original offset to radial truncation in the S&P rotation curves. Looking toward future studies of evolution in the TFR, we also provide a new calibration of the low-$z$ TFR designed for direct comparison with intermediate and high-$z$ data, based on a morphology-blind sample of bright emission-line galaxies. Within this sample, TF residuals vary systematically as a function of color and H$\alpha$ equivalent width.

## 1. Introduction

Two processes lie at the heart of galaxy evolution: mass assembly and star formation. For disk galaxies, the redshift-dependence of the correlation between rotation velocity and luminosity (a.k.a. the Tully-Fisher relation or TFR, Tully & Fisher 1977) offers a powerful probe of the evolving relationship between total mass and stellar light.

In the absence of mergers or significant accretion, galaxy masses are fixed, and luminosity evolution simply shifts the zero point of the TFR (or both the zero point and the slope, if faint galaxies show differential luminosity evolution relative to bright galaxies). Several studies have sought to measure luminosity evolution in the intermediate-$z$ TFR, motivated by the suggestion that the excess of faint blue galaxies in deep photometric surveys might indicate that galaxies were brighter in the past (Forbes et al. 1996; Rix et al. 1997; Simard & Pritchet 1998; Vogt et al. 1997; Bershady et al. 1999).

Conflicting results have emerged. Both Rix et al. (1997) and Simard & Pritchet (1998) measure apparent luminosity enhancements of ∼1.5–2 mag at $z \sim 0.3$, using samples selected for strong [OII] emission. However, Vogt et al. (1997) and Bershady et al. (1999) find much smaller zero point shifts at $z \sim 0.5$ and 0.3, respectively, using samples selected by morphology and color criteria less likely to bias the sample toward actively star-forming galaxies.

Our recent work on third-parameter dependences in the residuals of the TFR for a morphology-blind low-$z$ field galaxy sample (Kannappan et al. 2001a, hereafter KFF) motivates us to reexamine the intermediate-$z$ results. Most intermediate-$z$ TF studies have adopted the radio TF calibration of Pierce & Tully (1992) as a low-$z$ benchmark, but one would prefer a low-$z$ reference sample with optical rotation curves (like the higher $z$ samples) and a directly comparable method of distance determination,[1] to avoid systematic offsets arising from different analysis techniques. The low-$z$ data should also provide a statistically fair representation of the full range of field galaxy morphologies, colors, and emission-line equivalent widths, permitting one to simulate the selection criteria of intermediate-$z$ studies and investigate how these criteria influence the TFR.

The recently completed Nearby Field Galaxy Survey offers exactly these features, along with B-band photometry suitable for comparison with intermediate-$z$ analyses (Jansen et al. 2000a,b; Kannappan et al. 2001b). In §2 we use the NFGS to recalibrate two existing intermediate-$z$ studies (Vogt et al. 1997; Simard & Pritchet 1998), attempting to match analysis techniques, selection criteria, and data quality. The Vogt et al. and Simard & Pritchet studies represent the two extremes of the luminosity evolution debate, and both employ spatially resolved rotation curves, facilitating direct comparison with the NFGS. In §3 we present a reference TF calibration for use in future studies of evolution in the TFR, based on a morphology-blind sample of NFGS emission-line galaxies brighter than $\mathrm{M_B^i} = -18$. We also provide calibrations of the dependence of TF residuals on effective $B - R$ color and global EW(H$\alpha$).

## 2. Recalibrating the Intermediate-Redshift TFR

Table 1 summarizes our recalibration of the evidence for luminosity evolution in the samples of Vogt et al. (1997, hereafter V97) and Simard & Pritchet (1998, hereafter S&P). Both samples were originally calibrated against Pierce & Tully (1992, hereafter PT92).

---

[1] Although Hubble-law distances suffer from high scatter at low-$z$, they offer the simplest choice if the goal is consistency. The Cepheid-calibrated TFR of Pierce & Tully (1992) has been compared with intermediate-$z$ data assuming $\mathrm{H_0} = 75$, but the Cepheid calibration implies a higher $\mathrm{H_0}$ (∼85). In principle, this error could be avoided by adjusting the assumed $\mathrm{H_0}$. However, uncertainties remain, because the zero point of a Cepheid-calibrated TFR depends primarily on the properties of the Cepheid-hosting galaxies, and these galaxies constitute neither a complete nor a statistically large sample.

Table 1. Recalibration of Offsets in the Intermediate-$z$ TFR

| | Vogt et al.[a] | Simard & Pritchet |
|---|---|---|
| redshift range | $0.15 < z < 0.99$, $<z> = 0.52$ | $0.26 < z < 0.43$, $<z> = 0.34$ |
| # of galaxies in sample/NFGS reference sample | 11/27 | 12/18 |
| offset from PT92 in author cosmology [b] | -0.07 | -1.83 |
| offset from PT92 in $\Lambda$-cosmology [b] | -0.21 | -2.03 |
| offset from NFGS in $\Lambda$-cosmology [b] | 0.01 | -1.24 |
| calibration difference | 0.22 | 0.79 |
| explained by (see text): | | |
| sample selection[c] | -0.22 | 0.20 |
| systematic zero point offset TP92−NFGS | 0.44[d] | 0.44[d] |
| lack of inclination correction | N/A | 0.30 |
| lack of extinction correction | N/A | -0.41 |
| P.A. misalignment | N/A | 0.26 |
| additional correction: | | |
| rotation curve truncation | N/A | 0.71 |
| final offset | 0.01 | -0.53 |

[a]N. Vogt has kindly provided updated magnitudes for this sample, which differ from those in Vogt et al. (1996, 1997) due to improved $k$ corrections and revised extinction corrections that more closely match those of Pierce & Tully (1992, PT92). Vogt et al. (1996, 1997) used the equations in Tully & Fouque (1985) to correct luminosities for all internal extinction, whereas PT92 used the same equations to correct luminosities for only the excess internal extinction beyond what would be observed at face-on inclination.

[b]$\Lambda$-cosmology: $H_0 = 75$, $\Omega_{\rm M} = 0.3$, $\Omega_\Lambda = 0.7$; Vogt et al.: $H_0 = 75$, $\Omega_{\rm M} = 0.1$, $\Omega_\Lambda = 0$ ; Simard & Pritchet: $H_0 = 75$, $\Omega_{\rm M} = 1$, $\Omega_\Lambda = 0$. NFGS data are corrected for Virgocentric infall as in KFF; typical corrections for the subsamples considered here are $\sim$0.1 mag.

[c]The sample selection offset is computed relative to an NFGS reference sample with the same luminosity, inclination, and PA restrictions as the customized reference sample but with no restriction on morphology or peculiarity (for V97) or on EW([OII]) (for S&P).

[d]The systematic zero point offset in each column is simply the remainder of the calibration difference after known differences are subtracted. About 0.3 mag of the total 0.44 mag discrepancy between the NFGS and PT92 probably arises from a systematic offset in the Cepheid calibration of PT92 (Tully & Pierce (2000) report an 0.3 mag discrepancy between the calibrators used in early studies and those added later, which they attribute to a statistical fluke); this offset implies that the Hubble constant appropriate for comparison with PT92 is $\sim$85. The small remaining offset probably reflects the mismatch between radio linewidths and optical rotation velocities, in this case specifically $V_{pmm}$. Barton et al. (2000) have also reported discrepancies between calibrations in the style of PT92 and calibrations based on samples analogous to the NFGS (e.g. their own data or that of Courteau 1997).

### 2.1. The Vogt et al. Sample

Figure 1 directly compares V97's 11-galaxy "high quality" sample (with revised magnitudes courtesy of N. Vogt, private communication) with a 27-galaxy low-$z$ reference sample defined by similar criteria. V97 select "undisturbed spirals," which we interpret to mean all Sa–Sd spirals without strong bars or morphological peculiarities (warps, multiple nuclei, interacting companions, etc.; as identified in KFF). We exclude NFGS galaxies fainter than the faintest galaxy in the V97 sample ($\sim$$\mathrm{M}_{\mathrm{B}}^{i} = -19$). V97's "high quality" sample maintains slit P.A. misalignment $\Delta$P.A. $< 20$ and inclination $i > 30$; we tighten the latter restriction to $i > 40$ for the NFGS (tightening the restriction eliminates one galaxy, a $>3\sigma$ outlier from the low-$z$ TFR). Following V97, we calculate inclinations using $\cos i = b/a$ (N. Vogt, private communication) and adopt the extinction corrections of Tully & Fouque (1985). Both data sets are converted to the currently popular $\Lambda$-cosmology ($H_0 = 75$, $\Omega_{\mathrm{M}} = 0.3$, $\Omega_{\Lambda} = 0.7$).

V97 determine rotation velocities by fitting their observed data to emission lines simulated from a grid of exponential disk models with different terminal velocities, convolved with model seeing and masked with a model slit. Rather than directly reproduce their methods, we explore the range of plausible rotation velocities consistent with the NFGS data using three different circular-velocity estimation techniques: the "probable min-max" velocity $V_{pmm}$ (adapted from Raychaudhury et al. 1997, see KFF for details), the maximum velocity $V_{max}$, and the velocity determined from a fitted analytic rotation curve model $V_{fit}$ (see KFF). Figure 1 and Table 1 show results using $V_{pmm}$; this parameter makes no *a priori* assumptions about rotation curve shape and produces the best match with HI linewidths for the NFGS. Fixing the intermediate-$z$ slope to the value fitted to the low-$z$ data, we measure V97-minus-NFGS luminosity offsets of $+0.01 \pm 0.16$, $-0.21 \pm 0.15$ mag, and $+0.16 \pm 0.16$ mag using $V_{pmm}$, $V_{max}$, and $V_{fit}$ respectively. Clearly the systematic uncertainties associated with mismatched rotation curve analysis techniques are at least as large as the formal statistical errors. Nonetheless, all techniques are consistent with a null offset.[2]

These results broadly confirm the conclusions of V97 using a more appropriate reference sample than PT92. Vogt et al.'s calibration against PT92 yields $-0.21$ mag of luminosity evolution in our standard $\Lambda$-cosmology (Table 1). While not large, the offset between the two calibrations underscores the importance of standardizing sample selection and analysis techniques. The 0.22 mag difference between Vogt et al.'s calibration and our recalibration (computing NFGS rotation velocities with the preferred $V_{pmm}$ parameter) arises from a combination of partially canceling offsets due to both sample selection (the exclusion of barred, interacting, and non-spiral galaxies) and also a systematic zero point shift between PT92 and the NFGS.

[2]The V97 galaxies were selected for morphology, not color. However, the resulting sample is $\sim$0.2–0.3 mag bluer in $B-R$ color (using $(B-R) = 0.3 + 1.4(B-V)$) than the 27-galaxy NFGS comparison sample, implying a "reverse" luminosity offset in the R-band TFR. Such a reverse offset could indicate evolving stellar mass fraction (e.g. Buchalter et al. 2001), but the color offset is too small to rule out systematic errors from band-shifting and $k$-corrections.

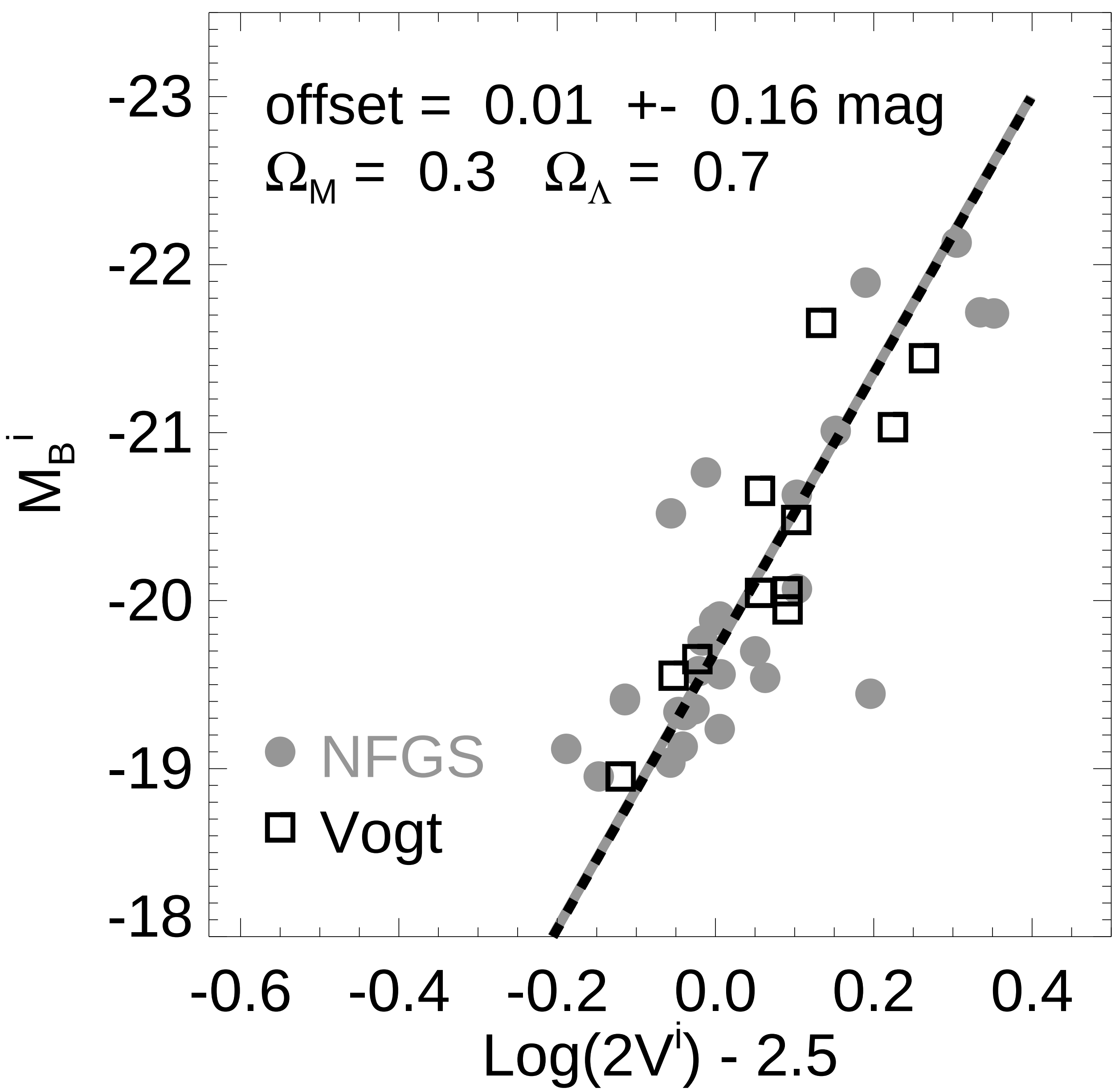


Fig. 1.— Direct comparison of the intermediate-$z$ sample of Vogt et al. (1997) and an NFGS subsample selected according to these authors' criteria. Intermediate-$z$ data (open squares) were provided courtesy of N. Vogt, private communication, and include revised extinction and $k$-corrections. We use only the "high-quality" sample from V97 and restrict our own sample by analogy. The gray line shows an inverse fit to the NFGS data (i.e. minimizing residuals in $\log 2V^i_{pmm}$), while the black dotted line shows a fit to the V97 data with slope fixed to the NFGS value.

### 2.2. The Simard & Pritchet Sample

Whereas Vogt et al. select galaxies primarily by morphology, Simard & Pritchet (1998, hereafter S&P) select bright galaxies with strong [OII] 3727 emission (EW([OII]) $< -20$) to make it easier to obtain kinematic measurements. For comparison with their 12-galaxy "kinematically normal" sample, we define a sample of 18 NFGS galaxies with EW([OII]) $< -20$, luminosity no fainter than the faintest S&P galaxy ($\sim$M$_{\rm B} = -18.5$), and $i > 40$ ($b/a < 0.78$). Note that S&P do not measure or correct for galaxy inclination angles; our $i > 40$ cut is an attempt to quantify S&P's selection preference for galaxies with some sign of elongation. With the $i > 40$ cut, the NFGS subsample has average inclination $<i> = 68$.

Figures 2a and 2b show TF data for the NFGS and S&P samples, with magnitudes converted to $H_0 = 75$, $\Omega_{\rm M} = 0.3$, $\Omega_\Lambda = 0.7$. Following S&P, we plot the data without inclination or extinction corrections. Gray points in Figure 2a represent NFGS galaxies rejected from the comparison sample within the allowed luminosity range. X's in Figure 2b mark three S&P galaxies with severe slit P.A. misalignments; $V \sin i$ values for these galaxies have been boosted by 25 km s$^{-1}$ to compensate.[3]

We determine the zero point of the TFR for both samples with the slope fixed to $-7$ in the M$_{\rm B}$, $\log(V \sin i)$ coordinate system (approximately the value S&P use, as measured from their Figure 4). Like V97, S&P model their rotation curves using exponential disk simulations convolved with seeing and instrumental blurring; for comparison, we use the three velocity parameters $V_{pmm}$, $V_{fit}$, and $V_{max}$ (§2.1). Respectively, these three parameters yield S&P-minus-NFGS luminosity offsets of $-1.24 \pm 0.32$, $-1.12 \pm 0.32$, and $-1.54 \pm 0.31$; we show results using $V_{pmm}$ in Figure 2.

S&P measure an average offset of $-2.03$ mag relative to PT92 (converted to our standard $\Lambda$-cosmology). Our measured offset differs from this value for several reasons, summarized in Table 1. First, our sample includes S&P's EW([OII]) restriction, which shifts the reference calibration toward higher luminosity by 0.20 mag. Unlike the PT92 calibration, the NFGS calibration omits inclination and extinction corrections to match S&P's analysis; these omissions shift the reference calibration toward higher and lower luminosity respectively, by 0.30 mag and $-0.41$ mag. Our P.A. misalignment correction on the S&P data reduces the apparent luminosity offset by 0.26 mag. Finally, we again see the systematic zero point shift between TP92 and the NFGS discussed in §2.1.

However, we have not yet addressed data quality. Figure 2c shows the effect of degrading the NFGS rotation curves to the average S/N level of the kinematically normal S&P data (8.16, using S&P's integrated S/N measurements computed within $\pm 3r_d$). To achieve roughly the same S/N, we add all the line signal from our H$\alpha$ rotation curves within $\pm 3r_d$, then artificially increase the

[3]The final S&P sample omits galaxies with $\Delta$P.A. $\geq 45°$ but still contains three galaxies with severe misalignments of $\sim$ 35–40°. To avoid discarding data from an already small sample, we retain these galaxies and attempt to compensate for their misalignments. S&P comment that misalignment probably reduces $V \sin i$ by about 25 km s$^{-1}$ for one of the galaxies, based on a numerical simulation. In the absence of further information, we add this number to all three galaxies' $V \sin i$ values. All 18 galaxies in the NFGS comparison sample have $\Delta$P.A. $< 5°$.

per-pixel rms noise $\sigma_{pix}$ within a box bounded by $\pm 3r_d$ and the minimum and maximum measured velocities. Choosing $\sigma_{pix}$ to give an overall S/N of 8.16 for the box, we next reevaluate the S/N of the individual points in the rotation curve, for each point summing the signal and the noise in the spectral line within the range of pixels where the signal exceeds the noise.

Finally, we truncate the rotation curve at the largest radius on each side with S/N equal to a fixed detection limit (Figure 3). As different rotation curve analysis algorithms differ in their detection efficiency, we vary this detection limit through a range of values: $\mathrm{S/N_{limit}} = 1.0$, 1.5, 2.0, 2.5. Applying these detection limits, we measure false luminosity offsets in the NFGS reference sample of $-0.43$, $-0.67$, $-0.71$, and $-1.51$ mag respectively (the $\mathrm{S/N_{limit}} = 2$ simulation result is shown in Figure 2c). As the $1.0\sigma$ limit seems optimistic, and the $2.5\sigma$ limit produces outliers more extreme than those seen in the S&P sample, we conclude that an offset of $\sim$0.7 mag is likely.[4] Figure 2c shows that this level of truncation may also contribute to S&P's observation of slightly higher offsets at the faint end of the TFR. The $\sim$0.7 mag offset corresponds to radial truncation at $\sim$1.7–$1.8r_d$, while a pure exponential disk first reaches peak velocity at $2.2r_d$ (Freeman 1970). For comparison, V97's rotation curves have average radial extent $\sim 3.0r_d$ and all reach at least $2.2r_d$ (N. Vogt, private communication).

If we subtract $\sim$0.7 mag from our measured luminosity offset of $-1.24$ mag, we are left with an offset of only $\sim -0.5$ mag. Furthermore, two effects we cannot easily quantify may act to reduce the offset even more. First, the cloud of gray points in Figure 2a shows that any lapse in maintaining high inclination angles may produce substantial false luminosity evolution. Given S&P's low-resolution images and selection of actively star-forming galaxies, some of the elongation they observe may be caused by tidal tails or close companions rather than truly edge-on inclinations. Second, we have modeled rotation curve truncation using the customized NFGS reference sample, which may not reproduce the properties of the S&P sample despite similar selection criteria. If the S&P sample contains galaxies with more radially concentrated emission-line intensity profiles than are found in the NFGS, then additional truncation may occur (cf. Barton et al. 2000). S&P partially address this issue by rejecting four anomalous galaxies with [OII] disk scale lengths $\sim$10–30 times smaller than their broadband scale lengths.[5][6] Such galaxies would be likely to give artificially low

---

[4]Simard & Pritchet (1999) perform simulations in which they apply their rotation curve analysis techniques to model data of varying S/N, and they conclude that their techniques can recover a galaxy's full rotation velocity at the S/N levels of the real data in S&P. However, Simard & Pritchet (1999) do not test their techniques on degraded real data, and they assume that a galaxy's radial emission-line intensity profile can be modeled with the same exponential disk law that describes the continuum emission from the disk. For a given integrated S/N, adding a central intensity enhancement to their model data would decrease the S/N in the outer parts of the model rotation curves.

[5]S&P also label three other galaxies as anomalous, but these appear to have been rejected for their P.A. misalignments rather than for centrally concentrated [OII] emission.

[6]With the caveat that our kinematics derive from H$\alpha$ rather than [OII], we find no evidence for such centrally concentrated emission within the 18-galaxy NFGS comparison sample. S&P's four anomalous galaxies tend toward higher luminosity than the rest of their sample. Comparably bright galaxies with EW([OII]) $< -20$ are rare in the

$V \sin i$ measurements, both because of rotation curve truncation and because of non-equilibrium gas motions associated with active nuclei (see the discussion of emission-line S0 galaxies in KFF). We conclude that the real luminosity offset in the S&P sample is probably $\lesssim$0.5 mag.

## 3. A Low-Redshift Reference Calibration

Here we provide a general-purpose low-$z$ reference calibration for use by future studies of evolution in the TFR. Such a calibration cannot include sample-specific details such as the effects of low S/N, but it can match the general properties of higher $z$ TF samples, which are nearly always field galaxy samples with optical emission-line rotation curves and Hubble-law distances.

Figure 4a shows the B-band TFR for a morphology-blind sample of 70 nearby galaxies. The sample includes all NFGS emission-line galaxies brighter than $\mathrm{M}_\mathrm{B}^i = -18$ and inclined by more than 40 degrees. As the NFGS provides a statistically representative sample of galaxies in the local universe, the subsample shown here provides a statistically representative sample of bright emission-line galaxies with $i > 40$. Full details of our parameter definitions, inclination and extinction corrections, error analysis, and fitting techniques are given in KFF. Distances are derived from a linear Hubble flow model with $\mathrm{H}_0 = 75$, corrected for Virgocentric infall. The superscript $i$ indicates corrections for inclination and internal extinction following the methods of Tully & Pierce (2000). For the extinction corrections, we convert the optical velocities to an equivalent radio linewidth scale as discussed in KFF.

Figures 4b & 4c display "third parameter" correlations between the residuals from the TFR in Figure 4a and both effective $(B - R)$ color and global EW(H$\alpha$); the caption also provides a fit to the much noisier TF residual–EW([OII]) correlation.[7] We discuss the physical drivers behind these correlations in KFF; here we present them simply as useful tools for evaluating the effect of selection biases on TF zero point (but one should bear in mind that the slopes or zero points of the correlations may themselves evolve with redshift). The color–TF residual correlation may also help to flag outlier galaxies that show apparent luminosity offsets for reasons unrelated to luminosity evolution, e.g. systematic errors or nuclear activity (Figure 4d).

---

NFGS, which fairly represents the general galaxy population (see KFF). The high fraction of anomalous galaxies in the S&P sample may be an artifact of their target ranking system, which prioritizes the brightest galaxies with the highest EW([OII]).

[7]Total colors and central-aperture equivalent widths do not predict TF residuals as well as effective colors and global equivalent widths. Total colors behave much like effective colors but are subject to greater measurement uncertainty (see KFF).

## 4. Discussion

The recalibrations and analysis presented here largely reconcile the results of V97 and S&P. Sample selection effects influence both samples, but we find much larger systematic offsets in the S&P sample, arising from both sample selection and data analysis issues. Our analysis leaves room for a small discrepancy between the two studies ($\lesssim$0.5 mag), which if present may reflect differential evolution for different galaxy types: S&P selected for actively star-forming galaxies, while V97 selected for undisturbed spirals.

Clearly, if we hope to understand the overall luminosity evolution of the general galaxy population, then neither of these samples tells the whole story. Furthermore, our measurements of luminosity evolution are fundamentally flawed, in that we have compared low-$z$ galaxies with intermediate-$z$ galaxies that have similar properties, rather than comparing low-$z$ galaxies with intermediate-$z$ galaxies that *will evolve to have* similar properties (i.e. our analysis suffers from "progenitor bias," in the language of van Dokkum & Franx 1996).

Without a full theory of galaxy evolution, the best way to address progenitor bias is to observe a broadly representative statistical sample. A survey equivalent to the full NFGS at higher redshift would allow us to evaluate the changing demographics of Tully-Fisher galaxies as well as their luminosity offsets. Future studies may also observe evolution in the slope or zero point of the color–TF residual correlation, another measure of global star formation history (see KFF). The reference calibrations presented here await such a study.

We thank Rolf Jansen and Nicole Vogt for providing data in electronic form, and Saurabh Jha, Warren Brown, and Betsy Barton for helpful discussions.

## REFERENCES

Barton, E. J., Geller, M. J., Bromley, B. C., van Zee, L., & Kenyon, S. J. 2000, in submitted

Bershady, M. A., Haynes, M. P., Giovanelli, R., & Andersen, D. R. 1999, in ASP Conf. Ser. 182: Galaxy Dynamics - A Rutgers Symposium, 499

Buchalter, A., Jimenez, R., & Kamionkowski, M. 2001, in Submitted to MNRAS, 5 pages, 3 figures., 2025+

Courteau, S. 1997, AJ, 114, 2402

Forbes, D. A., Phillips, A. C., Koo, D. C., & Illingworth, G. D. 1996, ApJ, 462, 89

Freeman, K. C. 1970, ApJ, 160, 811

Jansen, R. A., Fabricant, D., Franx, M., & Caldwell, N. 2000a, ApJS, 126, 331

Jansen, R. A., Franx, M., Fabricant, D., & Caldwell, N. 2000b, ApJS, 126, 271

Kannappan, S. J., Fabricant, D. G., & Franx, M. 2001a, in preparation

Kannappan, S. J., Fabricant, D. G., Franx, M., Berlind, P., Balog, Z., Carter, B., Hough, L. E., Lepore, N., & Weinberg-Wolf, J. 2001b, in preparation

Pierce, M. J. & Tully, R. B. 1992, ApJ, 387, 47

Raychaudhury, S., von Braun, K., Bernstein, G. M., & Guhathakurta, P. 1997, AJ, 113, 2046

Rix, H., Guhathakurta, P., Colless, M., & Ing, K. 1997, MNRAS, 285, 779

Simard, L. & Pritchet, C. J. 1998, ApJ, 505, 96

—. 1999, PASP, 111, 453

Tully, R. B. & Fisher, J. R. 1977, A&A, 54, 661

Tully, R. B. & Fouque, P. 1985, ApJS, 58, 67

Tully, R. B. & Pierce, M. J. 2000, ApJ, 533, 744

van Dokkum, P. G. & Franx, M. 1996, MNRAS, 281, 985

Vogt, N. P., Forbes, D. A., Phillips, A. C., Gronwall, C., Faber, S. M., Illingworth, G. D., & Koo, D. C. 1996, ApJ, 465, L15

Vogt, N. P., Phillips, A. C., Faber, S. M., Gallego, J., Gronwall, C., Guzman, R., Illingworth, G. D., Koo, D. C., & Lowenthal, J. D. 1997, ApJ, 479, L121

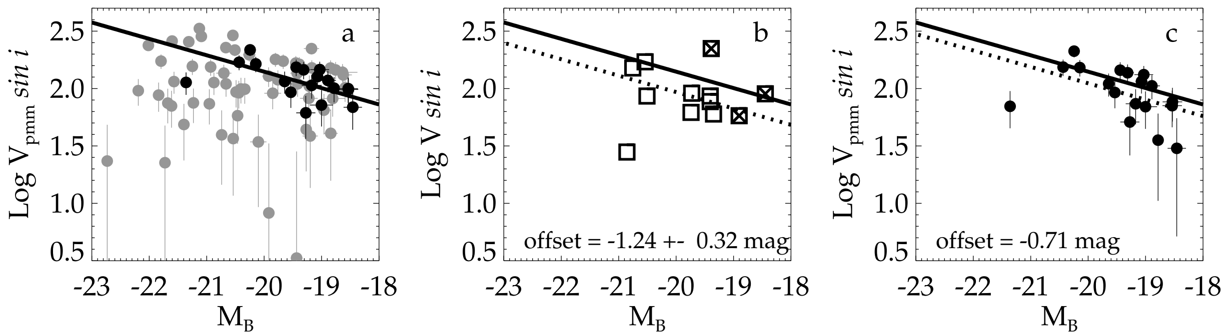


Fig. 2.— Comparison of "kinematically normal" galaxy data from Simard & Pritchet (1998) and data for an equivalent NFGS subsample. Following S&P, we plot the TFR without inclination or extinction corrections. (*a*) : The NFGS subsample. Black/gray points represent NFGS galaxies included/rejected by analogy with S&P, within roughly the same luminosity range as their sample. The solid line shows the best fit to the black points with slope fixed to $-7$. This line is repeated in each panel. (*b*) : The Simard & Pritchet sample. X's mark galaxies corrected for severe P.A. misalignment. The dotted line shows the best fit with slope fixed to $-7$. (*c*) : The same NFGS galaxies as in the left panel, but with the data degraded to simulate the radial truncation of the S&P data. The dotted line shows the best fit with slope fixed to $-7$.

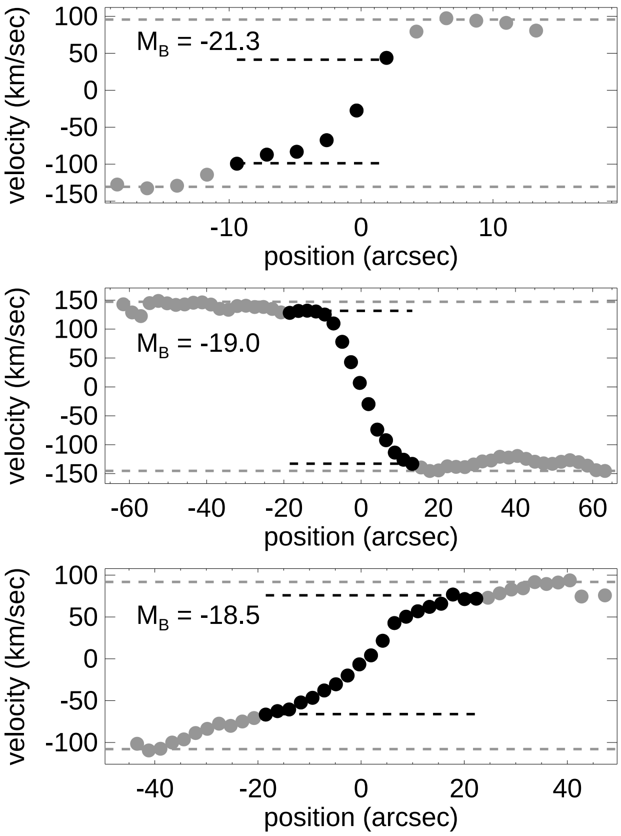


Fig. 3.— Simulated radial truncation of NFGS rotation curves induced by artificially degrading the S/N. Gray dots indicate the full extent of the original NFGS rotation curves, while black dots indicate those points that retain local S/N>2 when the integrated S/N is degraded to a value of 8.16 (the average integrated S/N of the rotation curves in S&P). Dashed lines indicate the velocity width $2V_{pmm}$ with and without truncation, uncorrected for inclination.

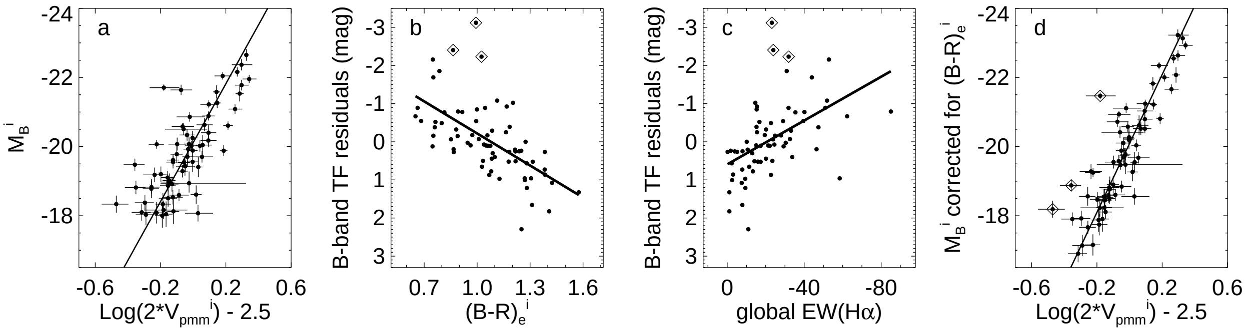


Fig. 4.— *a*) The TFR for a morphology-blind sample of emission-line galaxies brighter than $\mathrm{M}_\mathrm{B}^i = -18$. An unweighted inverse fit (minimizing velocity residuals) yields $\mathrm{M}_\mathrm{B}^i = -20.11 - 8.52(2V_{pmm}^i - 2.5)$. *b*) The correlation between TF residuals (relative to the fit in panel *a*) and effective $B-R$ color, i.e. color within the B-band half-light radius. An unweighted forward fit (minimizing residuals in the residuals) yields $\Delta\mathrm{M}_\mathrm{B}^\mathrm{i} = -3.0 + 2.8(\mathrm{B}-\mathrm{R})_\mathrm{e}^\mathrm{i}$. *c*) The correlation between TF residuals and global EW(H$\alpha$). An unweighted forward fit yields $\Delta\mathrm{M}_\mathrm{B}^\mathrm{i} = 0.59 + 0.029\mathrm{EW}(\mathrm{H}\alpha)$. Global EW([OII]) generates a noisier correlation, $\Delta\mathrm{M}_\mathrm{B}^\mathrm{i} = 0.55 + 0.031\mathrm{EW}([\mathrm{OII}])$. *d*) The color-corrected TFR, with magnitudes from panel *a* adjusted according to the fit in panel *b*. An unweighted inverse fit yields $\mathrm{M}_{\mathrm{B,corr}}^i = -20.09 - 9.97(2V_{pmm}^i - 2.5)$. Diamonds indicate outlier galaxies suspected of having large systematic inclination errors.